frontiers | Frontiers in Marine Science

TYPE Original Research
PUBLISHED 23 March 2023
DOI 10.3389/fmars.2023.1160371

OPEN ACCESS

EDITED BY
Jian Zhao,
Ocean University of China, China

REVIEWED BY
Yufeng Gong,
University of Toronto, Canada
Rui Zhang,
University of Jinan, China
Jonathan Hogarh,
Kwame Nkrumah University of Science and Technology, Ghana
Mohammed Serageldin,
Alexandria University, Egypt

*CORRESPONDENCE
Qing Luo
luoqingyt@126.com

SPECIALTY SECTION
This article was submitted to Marine Pollution, a section of the journal Frontiers in Marine Science

RECEIVED 07 February 2023
ACCEPTED 13 March 2023
PUBLISHED 23 March 2023

CITATION
Luo Q, Wang C, Gu L, Wu Z and Li Y (2023) Temporal trends of organophosphate esters in a sediment core from the tidal flat of Liao River estuary, Northeast China. *Front. Mar. Sci.* 10:1160371. doi: 10.3389/fmars.2023.1160371

Temporal trends of organophosphate esters in a sediment core from the tidal flat of Liao River estuary, Northeast China

Qing Luo*, Congcong Wang, Leiyan Gu, Zhongping Wu and Yujie Li

Key Laboratory of Regional Environment and Eco-Remediation of Ministry of Education, College of Environment, Shenyang University, Shenyang, China

The historical trends and inventory of organophosphate esters (OPEs) were investigated based on depth profiles of OPEs in sediment core collected from the tidal flat of the Liao River estuary in northeastern China. The concentration of $\sum_{13}$OPEs in sediment core has increased continuously since records began, reaching a peak of 10.8 ng g^{-1} dry weight (dw) in the 1960s, then began to decline and fall to a low of 3.91 ng g^{-1} dw in the 1980s, before rising again and increasing to 20.4 ng g^{-1} dw in the 2000s. After a brief decline, It started to increase again and reached a peak of 27.0 ng g^{-1} dw in 2018. Tributyl-n-phosphate was found in each layer of the sediment core, accounting for 31.9 - 100% of $\sum_{13}$OPEs. The fluxes of OPEs ranged from 46.5 to 105 ng cm^{-2} y^{-1} in the sediment layers deposited between 2007 and 2018. The inventory of OPEs in the sediment core was estimated to be 1541 ng cm^{-2}. This work reports for the first time the historical contamination trends of OPEs in Chinese sediments, which is important for assessing the environmental risk of OPEs.

KEYWORDS

organophosphate esters, sediment core, temporal trends, inventory, Liao River estuary

1 Introduction

Organophosphate esters (OPEs) were widely used in a variety of commercial items, including electronics, plastics, home decorations, and textiles, due to their outstanding flame retardant and plasticizing qualities and comparatively low cost (Wang X. et al., 2020). They were first used in the early 1900s and began to increase rapidly after the 1940s (USEPA, 1976). After the beginning of the 21st century, the use of OPEs expanded significantly as a result of the ban on polybrominated diphenyl ethers (PBDEs) (Stapleton et al., 2012). In 2018, 1.05 million tons of OPEs were consumed globally, making up more than 30% of all flame retardant consumption (Li T. Y. et al., 2019; Wang X. et al., 2020). However, a large body of evidence indicates that OPEs have adverse effects on the nervous system, reproductive system, immune system, and endocrine system (Noyes et al., 2015;

Hou et al., 2016; Zhou and Hu, 2017). As a result, environmentalists around the world are very concerned about OPEs as emerging contaminants.

OPEs are readily discharged into the environment because they are added as additives rather than chemically bound to the final product (Leisewitz et al., 2001). Relatively high concentrations of OPEs have recently been found in indoor and outdoor air, surface and ground water, sediment, and soil (Shi et al., 2016; Yadav et al., 2017; Luo et al., 2018a; Ji et al., 2019; Luo et al., 2021a). However, studies on the vertical distribution and historical contamination trends of OPEs in sediments have received little attention. Cao et al. (2017) investigated the contamination characteristics of OPEs in Lake Michigan sediment cores and found that OPEs date back to 1635. In sediment cores from the Palos Verdes Shelf off the coast of Los Angeles, which is heavily impacted by sewage treatment plant discharges, two peaks in OPEs concentrations occurred in the 1970s and 2000s (Li J. et al., 2019). In China, a major producer and consumer of OPEs, only the vertical distribution of OPEs in sediment cores taken from Taihu Lake (Ye et al., 2021; Zhang et al., 2022) and the coastal Laizhou Bay of the Bohai Sea (Wang et al., 2017) have been studied. The historical contamination trends of OPEs in Chinese sediments have not been reported because these existing studies did not date the sediment cores. Understanding the historical trends of contaminants in sediment cores is of great importance for estimating the inventory of contaminants and evaluating the risk of contaminants. Therefore, it is urgent to study the historical trends of OPEs in sediment cores in China.

To accurately understand the historical contamination trend of pollutants, the sampling locations of sediment cores must be chosen reasonably. The Liao River estuary is located at the top of Liaodong Bay, which is influenced by the Bohai Sea and the Liao River. The Bohai Rim has historically been a significant industrial hub and highly populated region of China, and there may be long-term emissions of OPEs. In addition, considerable concentrations of OPEs have been found in seawater and sediments of the Bohai Sea (Qi et al., 2021) and in water and sediment of the Liao River and Liao River estuary (Wang et al., 2015; Luo et al., 2020; Luo et al., 2021b). Therefore, it may be reasonable to collect sediment cores from the Liao River estuary and study the historical contamination trend of OPEs. Meanwhile, the Liao River estuary is often used as a study site for historical sedimentary patterns of geochemical components (Zhang et al., 2018; Chi et al., 2021).

In this study, 13 target OPEs were analyzed in sediment core layers obtained from the tidal flat of the Liao River estuary, and the deposition time of each layer was dated. The purposes of this study were to elucidate the historical contamination trend of OPEs and to estimate the deposition fluxes and inventory of OPEs.

2 Materials and methods

2.1 Sampling location and sample collection

The tidal flat of the Liao River estuary is a typical muddy tidal flat, which is located at the top of Liaodong Bay in China. It is formed by the steady accumulation of a large amount of silt brought into the estuary by the Liao River with the assistance of ocean currents and tidal currents. With the help of this continuous deposition, the temporal evolution of the contaminants can be studied. Therefore, a sediment core was obtained from the intertidal zone of the Liao River estuary on July 10, 2019, using a 150-cm-long manual coring tool (Figure 1). The length of this sediment core was 108 cm. The sediment core was cut into 2 cm layers using a stainless steel cutter, and a total of 54 samples were obtained. The samples were then brought to the laboratory in an ice bath, freeze-dried, homogenized, and stored at -20°C until further analysis was performed.

2.2 Dating of sediment core

The sediment core was delivered to the Public Technology Service Center of the Northeast Institute of Geography and Agroecology, Chinese Academy of Sciences, where they were age-dated by ^{210}Pb method utilizing a low-background g-ray spectrometer with a high pure Ge semiconductor (GWL-120-15-LB-AWT, ORTEC Instruments Ltd., Oak Ridge, TN, USA). The dry sediment samples were weighed and sealed in covered plastic test tubes before being tested for ^{210}Pb activity using 46.5 keV gamma emissions. After establishing the radioactive equilibrium (3 weeks), the emissions of ^{226}Ra with the 295 keV and 352 keV γ-rays radiated by its daughter nuclide ^{214}Pb were detected. The absolute efficiency of the detector was calibrated using standard sources and sediment samples of known radioactivity, both of which were obtained from the National Institute of Metrology in China. The counting time of ^{210}Pb was 16.7 h, with a measurement accuracy of 5 - 10% at the 95% confidence level. Assuming that in each sample, the supported ^{210}Pb and *in-situ* ^{226}Ra were in equilibrium, it is possible to calculate the unsupported ^{210}Pb activities (^{210}Pbex) using the difference between total ^{210}Pb and supported ^{210}Pb activity. The approximate ages of the sediments were then determined using the ^{210}Pbex and the constant rate of supply (CRS) model (Appleby and Oldfield, 1978). Sedimentation rates and sediment mass accumulation rates were calculated using the estimated ages, volume weights, and layer depths of sediments (Pratte et al., 2019).

2.3 Determination of OPEs concentrations

Using the method suggested in our previous studies (Luo et al., 2018b; Luo et al., 2018c), 13 OPEs were analyzed in sediment samples, including triethyl phosphate (TEP), tripropyl phosphate (TPP), tri-iso-butyl phosphate (TIBP), tributyl-n-phosphate (TNBP), tri(2-ethylhexyl) phosphate (TEHP), tri-butoxyethyl phosphate (TBOEP), tris-(2-chloroethyl) phosphate (TCEP), tris-(1-chloro-2-propyl) phosphate (TCIPP), tris[2-chloro-1-(chloromethyl) ethyl] phosphate (TDCPP), triphenyl phosphate (TPHP), 2-ethylhexyl diphenyl phosphate (EHDPP), tricresyl phosphate (TMPP), and triphenylphosphine oxide (TPPO). Briefly, 10 g of freeze-dried sediment sample was weighed and mixed with 20 ng of internal standards (TNBP-d_{27} and TPHP-d_{15}).

The mixture was then transferred to an extraction cell preloaded with 2 g of copper granules activated by diluted HCl and 2 g of silica gel activated by heat. The extraction cell was loaded into the ASE 300 (Dionex, USA) and run under the following conditions: the extractant was the 1:1 mixture of n-hexane and acetone; the extraction temperature, pressure, and time were set to 100°C, 1500 psi, and 10 min, respectively; the flush volume was set at 60% of the cell volume; the number of static extraction cycles was set to 2. The extract obtained by accelerated solvent extraction was then blown almost dry with nitrogen and redissolved with 1 mL of n-hexane for GC-MS/MS (Trace 1300 - TSQ 8000 Evo, Thermo Fisher, USA) analysis.

For the GC-MS/MS analysis, the pulse splitless injection mode was used and the injection volume was set to 1μL. Chromatographic separation was carried out using a TG-5SILMS column (30 m × 0.25μm × 0.25 mm, Thermo Fisher, USA) with the helium flow rate adjusted to 1 mL min^{-1}. The column's temperature was first set to 50°C and maintained for 1 min, raised to 180°C at 10°C min^{-1}, maintained for 8 min, raised to 240°C at 20°C min^{-1}, maintained for 8 min, raised to 255°C at 3°C min^{-1}, and then raised to 300°C at 30°C min^{-1}, maintained for 5 min. The temperatures of the injection port, transmission line, and ion source were set to 250, 280, and 280°C, respectively. The target OPEs were measured using the multiple reaction monitoring scanning mode, and Table S1 shows the pertinent characteristics, including the precursor ion, product ion, and collision energy.

2.4 QA/QC

Brown glass containers were used throughout the analysis to prevent photolysis of OPEs. To lower the background levels of OPEs, all brown glass containers were roasted at high temperatures and cleaned with acetone and n-hexane before use. The internal standard method was used to calculate the concentration of OPEs in samples. The method detection limits (MDLs) and quantitation limits (MQLs) were equal to 3 and 10 times the standard deviation obtained from the analysis of 8 blank spiked samples, respectively (USEPA, 1986), and are shown in Table S1.

Table S1 shows, which were determined by evaluating eight blank spiked samples and were, respectively, 3 and 10 times the standard deviation (USEPA, 1986). A procedural blank sample, a blank spiked sample, and a matrix spiked sample were included in the analytical process for every 10 real samples. Some OPEs were detected in the procedural blank samples, but their concentrations were lower than MDLs or MQLs. The concentrations of OPEs in the real samples were corrected by subtracting the blank values to eliminate the interference of background pollution. The spiked recoveries of OPEs ranged from 82.5% to 104%, and the RSDs were less than 12%.

2.5 Calculation of deposition flux and inventory

The deposition flux (ng cm^{-2} y^{-1}) and inventory (ng cm^{-2}) of OPEs in the sediment core were computed as follows:

$$Flux_i = C_i \times \rho_i \times R_i \quad (1)$$

$$Inventory = \sum C_i \times \rho_i \times h_i \quad (2)$$

where C_i is the pollutant concentration in the sediment core layer i (ng g^{-1} dw), ρ_i is the dry bulk density of core layer i (g cm^{-3}), R_i is the sedimentary rate of core layer i (cm y^{-1}), h_i is the thickness of core layer i (cm).

2.6 Statistical analysis

The statistical analyses for this investigation were conducted using SPSS Statistics (IBM, version 18) and Microsoft Excel (Microsoft Office, 2010). The concentrations of individual OPE with concentrations below the MDLs are specified as zero in the figures and the calculation of Σ_{13}OPEs.

3 Results and discussion

3.1 Pollution levels and historical trends

Table 1 and Figure 2 show the concentrations of OPEs in the sediment core of the tidal flat of the Liao River estuary. TNBP was found in each layer of this sediment core. TEP, TPP, and TPPO were only found in the upper layers, and their detection frequencies were less than 30%. The detection frequencies of TIBP, TEHP, TBOEP, TCEP, TCIPP, TPHP, and TMPP were more than 87%, and they were only undetected in some samples in the middle and deeper layers. The total concentrations of OPEs in the sediment ranged from 0.45 to 27.0 ng g^{-1} dw with an average of 10.3 ± 5.32 ng g^{-1} dw. Among them, the alkyl-OPEs consisting of TEP, TPP, TIBP, TNBP, TEHP, and TBOEP had the highest concentration of 0.45 to 15.6 ng g^{-1} dw with an average of 7.79 ± 3.56 ng g^{-1} dw, accounting for 75.6% of Σ_{13}OPEs. The Cl-OPEs consisting of TCEP, TCIPP, and TDCPP ranked second, accounting for 16.2% of Σ_{13}OPEs. Their concentrations ranged from nd to 9.23 ng g^{-1} dw, with an average of 1.67 ± 1.60 ng g^{-1} dw. TNBP and TCIPP were the most abundant monomers in alkyl- and Cl-OPEs with average concentrations of 4.87 ± 2.23 ng g^{-1} dw and 0.94 ± 1.11 ng g^{-1} dw, respectively.

The pollution levels of OPEs in the sediment core of the tidal flat of the Liao River estuary were lower than those found in sediment cores taken from the coastal Laizhou Bay of the Bohai Sea, China (CA: 11.2 - 102 ng g^{-1} dw, CB: 6.65 - 41.5 ng g^{-1} dw) (Wang et al., 2017) and the Taihu Lake, China (C1, 34.3 - 332 ng g^{-1} dw; C2, 30.1 - 117 ng g^{-1} dw) (Zhang et al., 2022). However, the detection frequencies of various OPEs in these three studies were comparable. For instance, sediment cores collected from the coastal Laizhou Bay (Wang et al., 2017) and Taihu Lake (Zhang et al., 2022) revealed the presence of TNBP, TCEP, TCIPP, and TPHP in all layers, which is consistent with the detection features of these compounds in the current study. The OPEs concentrations in this study were lower than those in the sediment core from southern Lake Michigan (M009, 1.74 - 41.4 ng g^{-1} dw), but comparable to

TABLE 1 The concentrations of OPEs in the sediment core (ng g^{-1} dw).

OPEs	Min	Max	Median (n=54)	Mean (n=54)	SD (n=54)	Fr*
TEP	nd*	0.73	nd	0.08	0.16	27.8%
TPP	nd	1.15	nd	0.07	0.21	22.2%
TIBP	nd	2.43	0.96	0.91	0.68	92.6%
TNBP	0.45	10.0	4.76	4.87	2.23	100%
TEHP	nd	1.71	0.64	0.61	0.36	88.9%
TBOEP	nd	3.02	1.30	1.26	0.72	90.7%
TCEP	nd	1.79	0.58	0.61	0.45	88.9%
TCIPP	nd	6.89	0.53	0.94	1.11	98.1%
TDCPP	nd	0.54	nd	0.12	0.18	33.3%
TPHP	nd	0.55	0.23	0.22	0.13	87.0%
EHDPP	nd	0.54	nd	0.10	0.14	44.4%
TMPP	nd	0.88	0.38	0.40	0.23	87.0%
TPPO	nd	1.02	nd	0.10	0.21	24.1%
∑Alkyl-OPEs	0.45	15.6	7.45	7.79	3.56	
∑Cl-OPEs	nd	9.23	1.30	1.67	1.60	
∑Aryl-OPEs	nd	1.36	0.80	0.72	0.36	
Σ_{13}OPEs	0.45	27.0	9.67	10.3	5.32	

*nd: Below the MDLs; Fr: Frequency of detection (%).

those in the sediment cores from central (M024, 1.27 - 19.9 ng g^{-1} dw) and northern (M047, 0.60 - 20.9 ng g-1 dw) Lake Michigan (Cao et al., 2017). According to Cao et al. (2017), TIBP, TNBP, TBOEP, and TCIPP had high detection frequencies in the three sediment cores from Lake Michigan, which is similar to the present study. However, TEP and TPP were not detected, even in the surface layer (Cao et al., 2017). This may be connected to the local OPEs' use and emission characteristics. For instance, the concentrations of OPEs in the sediment cores of the Palos Verdes Shelf off the coast of Los Angeles (0.68 - 1064 ng g^{-1} dw) were much greater than elsewhere in this investigation due to the impact of wastewater treatment plant effluents (Li J. et al., 2019).

Figure 2 shows the vertical distribution and historical trends of OPEs in the sediment core of the tidal flat of the Liao River estuary. As can be seen from the figure, OPEs can be detected in the sediments with a deposition time of 1569, however only TNBP. TIBP, TNBP, TBOEP, and TCIPP can be found in sediment cores from central Lake Michigan dating back to 1635 (Cao et al., 2017), but this does not imply that OPEs were used or released in the 1600s. One reason is the lack of production and usage records of OPEs before 1900, and another is that a large fraction of OPEs with log K_{oc}< 3.5 are present in pore water, which facilitates their migration to deeper sediment (Cao et al., 2017). Therefore, it is difficult to determine whether those OPEs with log K_{oc} less than 3.5 in sediments deposited before 1900 are caused by direct discharge or vertical migration, such as TNBP in the present study. However, given that OPEs have been used for more than 150 years (Van der Veen and De Boer, 2012), the presence of TIBP, TNBP, and TCIPP in the sediment with a deposition time of 1905 may be the result of a combination of direct discharge and vertical migration. After 1905, more kinds of OPE were detected, and the concentration of Σ_{13}OPEs likewise increased until it peaked in the 1960s at 10.8 ng g^{-1} dw. This peak may be attributed to the modest use of OPEs as flame retardants dating back to the 1960s (Greaves and Letcher, 2017). It should be noted that some OPEs with a log K_{oc} greater than 3.5, including TEHP, TBOEP, TPHP, and TMPP, were detected in the sediments deposited in the 1960s. The log K_{oc} greater than 3.5 implies that these OPEs are difficult to vertical migration through the pore water, which indicates that OPEs in the sediments during this period were mainly derived from direct discharge. After the 1960s, the concentration of Σ_{13}OPEs started to go downhill and peaked in the 1980s at 3.91 ng g^{-1} dw. Following that, it started to rise and continued to do so until it peaked in the 2000s at 20.4 ng g^{-1} dw. This is primarily due to the ban on PBDEs and the rise in OPE use in the twenty-first century (Stapleton et al., 2012). After 2007, the concentration of Σ_{13}OPEs fluctuated erratically but overall rose as the deposition time shrunk. The maximum concentration of Σ_{13}OPEs, 27.0 ng g^{-1} dw, was found in the topmost layers. This is connected to the ongoing rise in OPE consumption over the past few years (Li T. Y. et al., 2019). The historical trends of OPEs in this study are similar to previous findings in sediment cores from Lake Michigan (Cao et al., 2017) and the Palos Verdes Shelf off the coast of Los Angeles (Li J. et al., 2019). This indicates that OPEs have been present in the environment for a long time, but they haven't gotten enough attention. Until recent years, the ban on PBDEs has led to a rapid

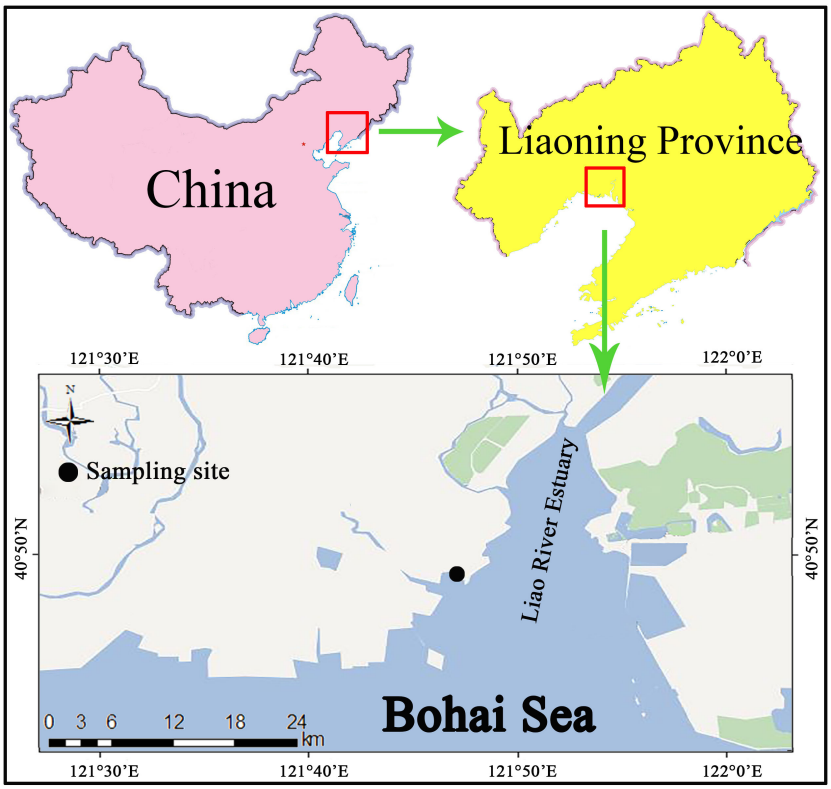

FIGURE 1
Sampling location.

increase in the production and use of OPEs as their primary substitutes (Stapleton et al., 2012). At the same time, the concentrations of OPEs in the environment have increased in tandem (Wang X. et al., 2020). Because of these, OPEs are currently receiving a lot of attention as emerging pollutants.

The historical trend of OPE monomers exhibits certain specific features. For instance, TEP and TPP were primarily detected in layers above 30 cm, with sediments corresponding to deposition periods from 2012 to 2018, indicating that TEP and TPP emissions had been present in this area since 2012. TEP and TPP are not found in the layers below 30 cm, which may be because they were less used and emitted in this area before 2012, but the more significant reason may be that they were easy to degrade (Wang Y. et al., 2020). In 1928, TCEP was discovered in sediments for the first time. Up to 1986, there was an overall upward trend in the content of TCEP in sediments, reaching a peak of 1.12 ng g^{-1} dw. The concentration then stayed low, averaging around 0.28 ng g^{-1} dw on average. Following the 2000s, the concentration of TCEP in sediments increased and remained between 1-2 ng g^{-1} dw. TCIPP first appeared in sediments in 1905, and after that, its concentration steadily increased until it peaked in 1960 at 2.01 ng g^{-1} dw. Since then, the concentration of TCIPP in the sediments had been low, with an average concentration of around 0.39 ng g^{-1} dw. After 2000, it started to increase. The concentration of TCIPP in sediment increased rapidly to 6.89 ng g^{-1} dw, especially in the last decade, and at a faster rate than TCEP. The main reason for the increase in the concentrations of TCEP and TCIPP in sediments over the last years is the widespread production and usage of OPEs (Van der Veen and De Boer, 2012). In addition, the 1980s showed a considerable increase in the production of TCIPP as an alternative to TCEP, which is why its concentration and growth rate are larger than that of TCEP (WHO, 1998). This is further supported by recent environmental monitoring data; TCIPP is the most frequently found OPE in environmental samples, with concentrations much greater than TCEP (Shi et al., 2016; Ji et al., 2019; Luo et al., 2020). TNBP, as the most predominant OPE, accounted for 47.3% of Σ_{13}OPEs and exhibited a historical trend comparable to that of Σ_{13}OPEs. Since TIBP is an isomer of TNBP and has similar chemical characteristics and applications, its historical trend is also comparable to that of TNBP. TPPO was only detected in sediments deposited after 2005. Since TPPO is difficult to biodegrade (Sternbeck et al., 2012), this suggested that the emission of TPPO in this region may have occurred after 2005. TEHP, TBOEP, TPHP, and TMPP were detected in all sediments deposited since the 1960s, but there was no noticeable trend in the variation of their concentrations. These four chemicals are hydrophobic (log *Koc* > 3.5), which makes them difficult to move down *via* pore water (Cao et al., 2017). This suggests that these four compounds may have been continuously discharged in this area after the 1960s. TDCPP and EHDPP were only found in a small number of sediment samples deposited before the year 2000, suggesting that they may not have been commonly used chemicals in this region at that time. However, as time went on, they were found in more sediment samples, and their concentrations increased, which indicated that TDCPP and EHDPP were used and released more frequently in the area after

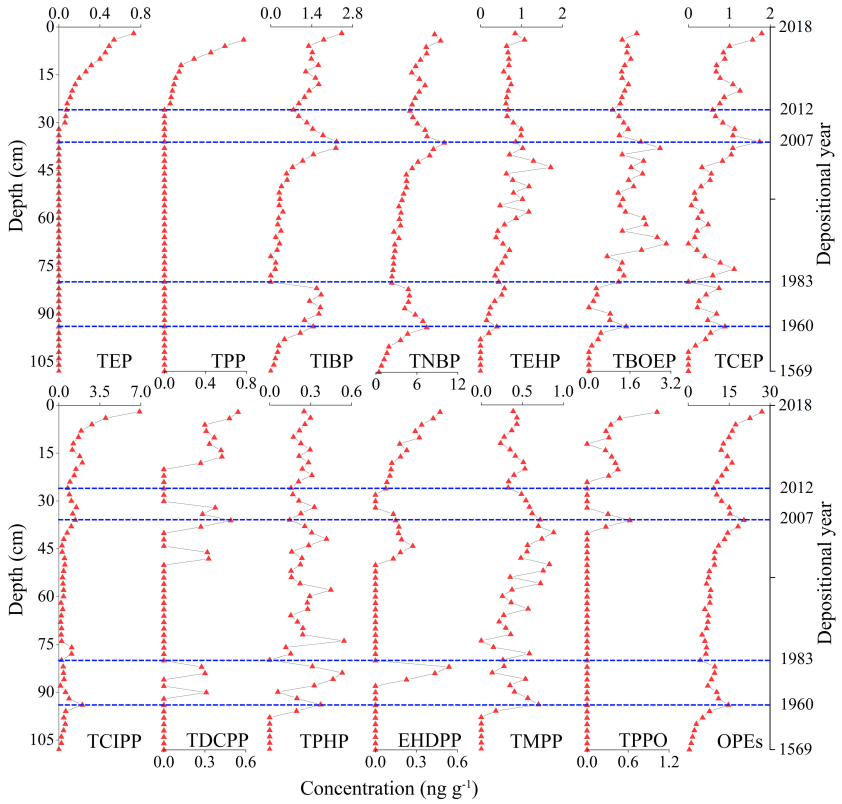

FIGURE 2
Historical trends of individual and total OPEs in the sediment core.

2000. In general, the vertical distribution of OPEs in sediment cores not only reflects information about their historical emissions but also relates to their characteristics, such as biodegradation and longitudinal mobility.

3.2 Composition characteristics

Figure 3 displays the composition profiles of OPEs in the sediment core of the tidal flat of the Liao River estuary. The majority of OPEs in the sediment core was alkyl-OPEs, accounting for 57.9 - 100% of $\sum_{13}$OPEs. They were followed by Cl-OPEs and aryl-OPEs with relative abundances of 0 - 34.2% and 0 - 14.4%, respectively. The relative abundance of TPPO was the lowest, only ranging from 0 to 3.79%. The individual OPE with the largest relative abundance was TNBP, accounting for 31.9 - 100% of $\sum_{13}$OPEs. TBOEP ranked second with a relative abundance of 0 - 41.8%. The relative abundances of TCIPP and TIBP were comparable, accounting for 0 - 25.5% and 0 - 23.5% of $\sum_{13}$OPEs, respectively. The relative abundances of TPP and TEP were the lowest, accounting for 0 - 4.27% and 0 - 2.82% of $\sum_{13}$OPEs, respectively. The OPE composition profiles in the sediment core and surface sediments of the Liao River estuary were similar. For instance, the order of relative contribution, i.e., alkyl-OPEs > CI-OPEs > aryl-OPEs (Luo et al., 2021b), was consistent with the present study. However, there were some differences. For example, the relative abundance of alkyl-OPE was lower than that of the present study, and the relative abundance of CI-OPE was higher than that of the present study (Luo et al., 2021b). The average relative abundance of TCIPP was 24.8% in the surface sediments collected from the Liao River estuary, which was the second most abundant OPE (Luo et al., 2021b). However, in this study, the average relative abundance of TCIPP was only 8.30%. TBOEP had the second-highest average relative abundance of OPE in the sediment core (12.7%), but its abundance in the surface sediments was lower (Luo et al., 2021b). This may be brought about by the long-term migration and transformation of OPEs in sediments, as well as the different pollution sources of OPEs in the Liao River estuary at various times.

The composition profiles of OPEs with different characteristics may be observed in sediment cores collected from different study regions. TMPP and TPHP accounted for 55.3% of $\sum_{10}$OPEs in the sediment core (C1) collected from the Palos Verdes Shelf off the coast of Los Angeles. The average relative abundances of TEP, TEHP, and TBOEP ranged from 11.0% to 14.2%. Several other OPEs, like TCIPP and TIBP, had relative abundances below 3.00% (Li J. et al., 2019). The relative abundances of TMPP and TBOEP were highest in the surficial 0 - 9.5 cm layers of sediment core (M024) collected from Lake Michigan, while TCIPP was the major OPE in the sediment below 9.5 cm (Cao et al., 2017). TBOEP and TNBP were the two most common OPEs in sediment core (C1) collected from Taihu Lake; their average relative abundances were 39.6% and 31.7%, respectively. TBOEP and TCIPP accounted for 27.0% and 26.8% of $\sum_{9}$OPEs, respectively, and were the most prevalent OPEs in sediment core (C2)

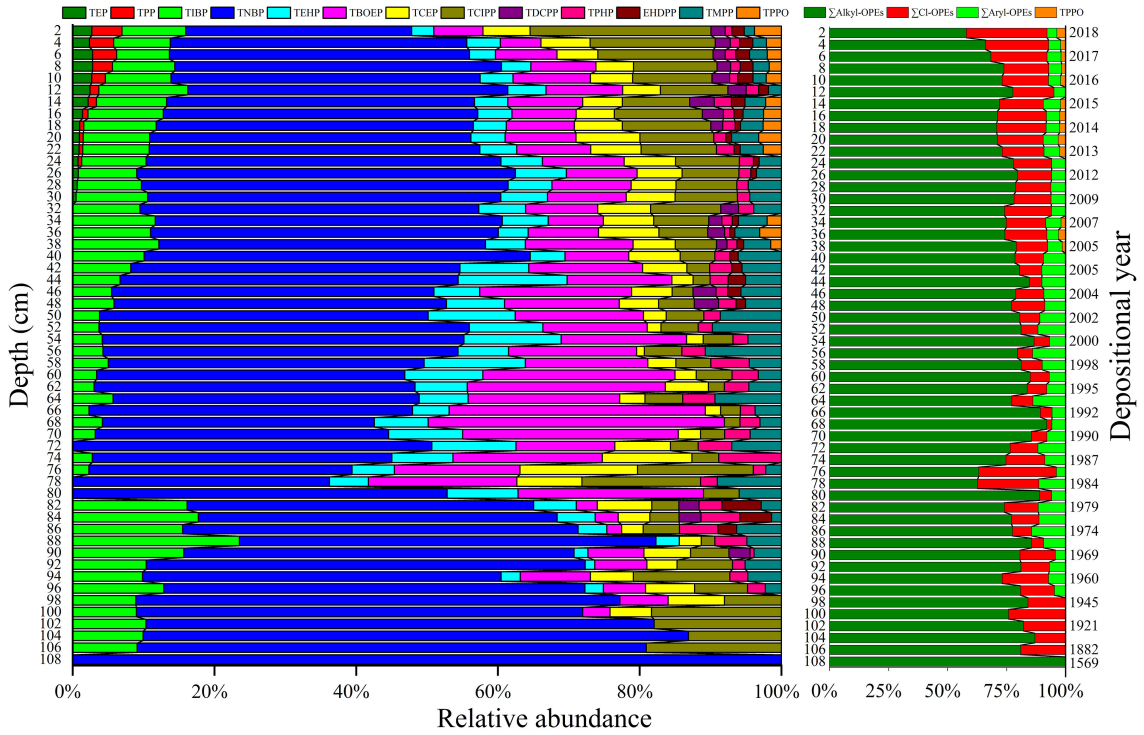

FIGURE 3
Profiles of OPEs in the sediment core at different depths.

(Zhang et al., 2022). Consistent with the results of this study, alkyl-OPEs were also the most prevalent OPEs in sediment cores collected from Taihu Lake, followed by aryl-OPEs and Cl-OPEs (Zhang et al., 2022). In the sediment cores of the coastal Laizhou Bay, TCIPP was the dominating OPE below 20 cm, followed by TCEP and TNBP. In the layers above 20 cm in the sediment core (CA), TNBP was the dominant OPE (Wang et al., 2017). However, the two most common OPEs in sediment core (CB) were TCIPP and TCEP, accounting for 16 - 40% and 7.6 - 53% of $\sum_8$OPEs, respectively (Wang et al., 2017). In the present study, TNBP was the most abundant OPE, followed by TBOEP, TCIPP, and TIBP. The differences in the composition profiles of OPEs were related to the usage and discharge characteristics of OPEs in different places at different times. TBOEP is commonly used in floor wax, vinyl plastics, and rubber stoppers, TCIPP is widely utilized in polyurethane foams, and TNBP is an important component of hydraulic power oil and fluid oil (Wang X. et al., 2020). The relatively high abundance of TNBP, TBOEP, and TCIPP in the sediment core may be due to a large number of related products discharged into the Liao River estuary.

3.3 Inventory

OPEs fluxes ranged from 46.5 to 105 ng cm^{-2} y^{-1} in sedimentary layers deposited between 2007 and 2018, from 13.4 to 66.3 ng cm^{-2} y^{-1} in sedimentary layers deposited between 1960 and 2007, and from 0.16 to 17.6 ng cm^{-2} y^{-1} in sedimentary layers deposited before 1960. The historical trends in the fluxes of OPEs and their concentrations in the sediment core were similar. This may be due to the stable sedimentation process in deep basins with fewer physical and biological mixing activities (Hoang et al., 2021). The OPEs inventory in this sediment core was estimated to be 1541 ng cm^{-2}. The OPE inventory in the sediment core from the tidal flat of the Liaohe River estuary was 9 - 40 times higher than that taken from Lake Michigan (38 - 178 ng cm^{-2}) (Cao et al., 2017). The deposition fluxes of OPEs in sediment cores collected from Lake Michigan were 0.01 - 1.23 ng cm^{-2} y^{-1} (Cao et al., 2017), which were lower than that of this study. The main reason for this may be the high sedimentation rate of tidal flat sediments in the Liao River estuary, ranging from 0.24 to 3.78 cm y^{-1} with an average value of 2.50 cm y^{-1}. Previous studies have indicated that the average sedimentation rates of sediments in the Liao River estuary were between 2.4 and 2.9 cm y^{-1} (Yang et al., 1993; Song et al., 1997; Liu et al., 2017), which is consistent with the results of this study.

4 Conclusions

In the present study, the sedimentary record of OPEs in the tidal flat of the Liao River estuary in northeast China was investigated. All sediment core layers included TNBP, however, only the upper layers had TEP, TPP, and TPPO. The concentrations of OPEs in the sediment core first increased, then decreased, and finally increased with the shortening of deposition time, which were related to the use and discharge of OPEs. The most abundant OPE is TNBP, followed by TBOEP, TCIPP, and TIBP. The deposition fluxes and OPE inventory in the sediment core of the tidal flat of the Liao River estuary are high because of the high sedimentary rate.

Data availability statement

The original contributions presented in the study are included in the article/Supplementary Material. Further inquiries can be directed to the corresponding author.

Author contributions

QL planned, supervised, prepared, and edited the manuscript. CW, LG, ZW, and YL executed the work. All authors contributed to the article and approved the submitted version.

Funding

This work was funded by the National Natural Science Foundation of China (NO. 41807384) and the Young and Middle-aged Scientific and Technological Innovation Talents Project of Shenyang (NO. RC220128).

Conflict of interest

The authors declare that the research was conducted in the absence of any commercial or financial relationships that could be construed as a potential conflict of interest.

Publisher's note

All claims expressed in this article are solely those of the authors and do not necessarily represent those of their affiliated organizations, or those of the publisher, the editors and the reviewers. Any product that may be evaluated in this article, or claim that may be made by its manufacturer, is not guaranteed or endorsed by the publisher.

Supplementary material

The Supplementary Material for this article can be found online at: https://www.frontiersin.org/articles/10.3389/fmars.2023.1160371/full#supplementary-material

References

Appleby, P., and Oldfield, F. (1978). The calculation of lead-210 dates assuming a constant rate of supply of unsupported 210Pb to the sediment. *Catena* 5, 1–8. doi: 10.1016/S0341-8162(78)80002-2

Cao, D., Guo, J., Wang, Y., Li, Z., Liang, K., Corcoran, M. B., et al. (2017). Organophosphate esters in sediment of the great lakes. *Environ. Sci. Technol.* 51 (3), 1441–1449. doi: 10.1021/acs.est.6b05484

Chi, G. X., Liu, B. L., Hu, K., Yang, J., and He, B. C. (2021). Geochemical Composition of sediments in the liao river estuary and implications for provenance and weathering. *Reg. Stud. Mar. Sci.* 45, 101833. doi: 10.1016/j.rsma.2021.101833

Greaves, A. K., and Letcher, R. J. (2017). A review of organophosphate esters in the environment from biological effects to distribution and fate. *Bull. Environ. Contam. Toxicol.* 98 (1), 2–7. doi: 10.1007/s00128-016-1898-0

Hoang, A. Q., Aono, D., Watanabe, I., Kuwae, M., Kunisue, T., and Takahashi, S. (2021). Contamination levels and temporal trends of legacy and current-use brominated flame retardants in a dated sediment core from beppu bay, southwestern Japan. *Chemosphere* 266, 129180. doi: 10.1016/j.chemosphere.2020.129180

Hou, R., Xu, Y. P., and Wang, Z. J. (2016). Review of OPFRs in animals and humans: Absorption, bioaccumulation, metabolism, and internal exposure research. *Chemosphere* 153, 78–90. doi: 10.1016/j.chemosphere.2016.03.003

Ji, Y., Wang, Y., Yao, Y. M., Ren, C., Lan, Z. H., Fang, X. G., et al. (2019). Occurrence of organophosphate flame retardants in farmland soils from northern china: primary source analysis and risk assessment. *Environ. pollut.* 247, 832–838. doi: 10.1016/j.envpol.2019.01.036

Leisewitz, A., Kruse, H., and Schramm, E. (2001). *Substituting Environmentally relevant flame retardants: Assessment fundamentals* (Berlin, Germany: Umweltbundesamt).

Li, T. Y., Bao, L. J., Wu, C. C., Liu, L. Y., Wong, C. S., and Zeng, E. Y. (2019). Organophosphate flame retardants emitted from thermal treatment and open burning of e-waste. *J. Hazard Mater* 367, 390–396. doi: 10.1016/j.jhazmat.2018.12.041

Li, J., Wang, J., Taylor, A. R., Cryder, Z., Schlenk, D., and Gan, J. (2019). Inference of organophosphate ester emission history from marine sediment cores impacted by wastewater effluents. *Environ. Sci. Technol.* 53, 8767–8775. doi: 10.1021/acs.est.9b01713

Liu, D. W., Hu, K., Zhao, X., Zhang, K. X., Gong, X. J., and Tang, G. W. (2017). The research of sedimentary environment of gaizhou shoal at liaohe estuary in recent 30 years. *Haiyang Xuebao* 39 (7), 131–142. doi: 10. 3969/j. issn. 0253-4193. 2017. 07. 013

Luo, Q., Gu, L., Wu, Z., Shan, Y., Wang, H., and Sun, L. N. (2020). Distribution, source apportionment and ecological risks of organophosphate esters in surface sediments from the liao river, northeast China. *Chemosphere* 250, 126297. doi: 10.1016/j.chemosphere.2020.126297

Luo, Q., Li, Y. J., Wu, Z. P., Wang, X. X., Wang, C. C., Shan, Y., et al. (2021a). Phytotoxicity of tris-(1-chloro-2-propyl) phosphate in soil and its uptake and accumulation by pakchoi (Brassica chinensis l. cv. SuZhou). *Chemosphere* 277, 130347. doi: 10.1016/j.chemosphere.2021.130347

Luo, Q., Shan, Y., Muhammad, A., Wang, S. Y., Sun, L. N., and Wang, H. (2018a). Levels, distribution, and sources of organophosphate flame retardants and plasticizers in urban soils of shenyang, China. *Environ. Sci. pollut. Res.* 25, 31752–31761. doi: 10.1007/s11356-018-3156-y

Luo, Q., Wang, S. Y., Shan, Y., Sun, L. N., and Wang, H. (2018c). Matrix solid-phase dispersion coupled with gas chromatography-tandem mass spectrometry for simultaneous determination of 13 organophosphate esters in vegetables. *Anal. Bioanal. Chem.* 410, 7077–7084. doi: 10.1007/s00216-018-1308-z

Luo, Q., Wang, S. Y., Sun, L. N., and Wang, H. (2018b). Simultaneous accelerated solvent extraction and purification for the determination of thirteen organophosphate esters in soils by gas chromatography-tandem mass spectrometry. *Environ. Sci. pollut. Res.* 25, 19546–19554. doi: 10.1007/s11356-018-2047-6

Luo, Q., Wu, Z. P., Wang, C. C., Gu, L. Y., Li, Y. J., and Wang, H. (2021b). Seasonal variation, source identification, and risk assessment of organophosphate ester flame retardants and plasticizers in surficial sediments from liao river estuary wetland, China. *Mar. pollut. Bull.* 173, 112947. doi: 10.1016/j.marpolbul.2021.112947

Noyes, P. D., Haggard, D. E., Gonnerman, G. D., and Tanguay, R. L. (2015). Advanced Morphological - behavioral test platform reveals neurodevelopmental defects in embryonic zebrafish exposed to comprehensive suite of halogenated and organophosphate flame retardants. *Toxicol. Sci.* 145, 177–195. doi: 10.1093/toxsci/kfv044

Pratte, S., Bao, K., Shen, J., De Vleeschouwer, F., and Le Roux, G. (2019). Centennial records of cadmium and lead in NE China lake sediments. *Sci. Total Environ.* 657, 548–557. doi: 10.1016/j.scitotenv.2018.11.407

Qi, Y. J., He, Z. S., Yuan, J. J., Ma, X. D., Du, J. Q., Yao, Z. W., et al. (2021). Comprehensive evaluation of organophosphate ester contamination in surface water and sediment of the bohai Sea, China. *Mar. Pollut. Bull.* 163, 112013. doi: 10.1016/j.marpolbul.2021.112013

Shi, Y. L., Gao, L. H., Li, W. H., Wang, Y., Liu, J. M., and Cai, Y. Q. (2016). Occurrence, distribution and seasonal variation of organophosphate flame retardants and plasticizers in urban surface water in Beijing, China. *Environ. pollut.* 209, 1–10. doi: 10.1016/j.envpol.2015.11.008

Song, Y. X., Zhan, X. W., and Wang, Y. G. (1997). Modern sedimentation characteristics of estuary region of the liaodong bay. *Haiyang Xuebao* 19 (5), 145–149.

Stapleton, H. M., Sharma, S., Getzinger, G., Ferguson, P. L., Gabriel, M., Webster, T. F., et al. (2012). Novel and high volume use flame retardants in US couches reflective of the 2005 pentaBDE phase out. *Environ. Sci. Technol.* 46, 13432–13439. doi: 10.1021/es303471d

Sternbeck, J., Hel´en Osterås, A., and Woldegiorgis, A. (2012). *Screening of TPPO, TMDD and TCEP, three polar pollutants* (Stockholm, Sweden: Swedish Environmental Protection Agency).

USEPA (1976). *The manufacture and use of selected aryl and alkyl aryl phosphate esters (Task I), EPA 560/6-76-008*. (US Environmental Protection Agency (EPA)). Available at: https://nepis.epa.gov/.

USEPA (1986) *EPA Regulation 40 CFR part 136 (appendix b) appendix b to part 136 d definition and procedure for the determination of the method detection limitd revision 1.11* (US Environmental Protection Agency (EPA). Available at: http://www.ecfr.gov/ (Accessed 5 March 2013).

Van der Veen, I., and De Boer, J. (2012). Phosphorus flame retardants: properties, production, environmental occurrence, toxicity and analysis. *Chemosphere* 88, 1119–1153. doi: 10.1016/j.chemosphere.2012.03.067

Wang, R., Tang, J., Xie, Z., Mi, W., Chen, Y., Wolschke, H., et al. (2015). Occurrence and spatial distribution of organophosphate ester flame retardants and plasticizers in 40 rivers draining into the bohai Sea, north China. *Environ. pollut.* 198, 172–178. doi: 10.1016/j.envpol.2014.12.037

Wang, Y., Wu, X. W., Zhang, Q. N., Hou, M. M., Zhao, H. X., Xie, Q., et al. (2017). Organophosphate esters in sediment cores from coastal laizhou bay of the bohai Sea, China. *Sci. Total Environ.* 607-608, 103–108. doi: 10.1016/j.scitotenv.2017.06.259

Wang, Y., Yao, Y. M., Han, X. X., Li, W. H., Zhu, H. K., Wang, L., et al. (2020). Organophosphate di- and tri-esters in indoor and outdoor dust from China and its implications for human exposure. *Sci. Total Environ.* 700, 134502. doi: 10.1016/j.scitotenv.2019.134502

Wang, X., Zhu, Q. Q., Yan, X. T., Wang, Y. W., Liao, C. Y., and Jiang, G. B. (2020). A review of organophosphate flame retardants and plasticizers in the environment: Analysis, occurrence and risk assessment. *Sci. Total Environ.* 731, 139071. doi: 10.1016/j.scitotenv.2020.139071

WHO (1998). *Environmental health criteria 209, flame retardants: Tris(chloropropyl) phosphate and Tris(2-chloroethyl) phosphate* (Geneva, Switzerland: World Health Organization).

Yadav, I. C., Devi, N. L., Zhong, G., Li, J., Zhang, G., and Covaci, A. (2017). Occurrence and fate of organophosphate ester flame retardants and plasticizers in indoor air and dust of Nepal: implication for human exposure. *Environ. pollut.* 229, 668–678. doi: 10.1016/j.envpol.2017.06.089

Yang, S. L., Liu, G. X., Du, R. Z., and Zhang, B. (1993). Study on the modern sedimentation rate through 210Pb age dating, liaodong bay. *Acta Sedimentol. Sin.* 11 (1), 128–135.

Ye, L. J., Meng, W. K., Huang, J. N., Li, J. H., and Su, G. Y. (2021). Establishment of a target, suspect, and functional GroupDependent screening strategy for organophosphate esters (OPEs): "Into the unknown" of OPEs in the sediment of taihu lake, China. *Environ. Sci. Technol.* 55, 5836–5847. doi: 10.1021/acs.est.0c07825

Zhang, W. P., Guo, C. S., Lv, J. P., Li, X., and Xu, J. (2022). Organophosphate esters in sediment from taihu lake, China: Bridging the gap between riverine sources and lake sinks. *Front. Environ. Sci. Eng.* 16 (3), 30. doi: 10.1007/s11783-021-1464-9

Zhang, K., Pan, S., Liu, Z., Li, G., Xu, Y., and Hao, Y. (2018). Vertical distributions and source identification of the radionuclides ^{239}Pu and ^{240}Pu in the sediments of the liao river estuary, China. *J. Environ. Radioact.* 181, 78–84. doi: 10.1016/j.jenvrad.2017.10.016

Zhou, Q. X., and Hu, X. G. (2017). Systemic stress and recovery patterns of rice roots in response to graphene oxide nanosheets. *Environ. Sci. Technol.* 51 (4), 2022–2030. doi: 10.1021/acs.est.6b05591